Ocean Engineering 266 (2022) 112710

Contents lists available at ScienceDirect

Ocean Engineering

journal homepage: www.elsevier.com/locate/oceaneng

Robust tracking control for dynamic positioning ships subject to dynamic safety constraints

Yeye Liu [a,*], Xiaogong Lin [a], Kun Liang [b]

[a] College of Intelligent Systems Science and Engineering, Harbin Engineering University, Harbin, 150001, China
[b] School of Intelligent Engineering, Zhengzhou University of Aeronautics, Zhengzhou, 450046, China

ARTICLE INFO

Keywords:
Dynamic positioning ships
Trajectory tracking
Sliding mode disturbance observer (SMDO)
Unified barrier function (UBF)
Bioinspired neurodynamics model (BNDM)

ABSTRACT

This paper addresses the dynamic safety constraint problem for the Dynamic Positioning (DP) ship subject to model uncertainties and unknown environmental disturbances. To guarantee the dynamic safety constraints, a new constraint technique based on the unified barrier function (UBF) is used to convert the original constrained DP system into an equivalent "non-constrained" one. By blending the new coordinate transformation into backstepping design, the position and velocity of the DP ship keep within the given constraints. In addition, a bioinspired neurodynamics model (BNDM) is developed to solve the traditional differential explosion problem of the virtual control law and limit the output in a certain range. Further, a sliding mode disturbance observer (SMDO) is introduced to estimate the model uncertainties and unknown environmental disturbances with minor chattering and rapid convergence. Finally, the effectiveness of the proposed controller and observer of the DP ship is illustrated by numerical simulations.

1. Introduction

With the increasing demand for offshore exploration and marine energy development, dynamic positioning systems have been widely used as autonomous control systems for ship operations (Fossen, 2011). The dynamic positioning system keeps the ship's position and heading at the desired value by controlling the ship's thrusters (Kulczycki et al., 2021). Over the year, numerous tracking control methods with the uncertainties have been developed over the years, such as adaptive backstepping control (Lu et al., 2021), neural network-based intelligent control (Li et al., 2022b), sliding mode control (Zhang et al., 2022), disturbance rejection control (Zheng et al., 2022a), and output feedback control (Ghommam et al., 2022). The DP ship is known as a highly non-linearity system, whose dynamics model parameters including hydrodynamic coefficients are very difficult to know accurately. And it is inevitable that the DP ship is influenced by environmental disturbances. (Fossen, 2011). These factors make the design of high-performance tracking controller design challenging. In addition, the demand for the safety state (position and velocity) constraints in the DP ship operation is growing rapidly. Once these constraints are ignored, the tracking performance of the DP ship can be affected and even collision can occur (Du et al., 2015). However, the above control methods cannot ensure that the state of the DP ship is within the safe region in practical operations, and literature on the DP ship's controller design with dynamic asymmetric state constraints are limited. Hence, it is necessary to study tracking control strategies for the DP ship with the state safety constraints and disturbance rejection.

Barrier Lyapunov function (BLF) is an effective method to deal with the state safety constraint issue of the DP ship in recent years. The BLF-based constraint control approach ensured that the DP ship was in the desired region by assigning a large value to Lyapunov when the DP ship started to approach the boundary (Tee and Ge, 2011). In He et al. (2016), an asymmetric BLF was introduced to handle output constraint of the marine vessel. Kong et al. (2018) designed an asymmetric time-varying BLF to ensure that the state of the marine vessel was bounded by the considered constraint function. Qin et al. (2020) designed a tan-type BLF-based tracking controller for the unmanned surface vessel to ensure that the error variables were kept within predefined limits. Wang et al. (2021) investigated a time-varying tan-type BLF for tracking error constraints of unmanned surface vehicles. However, BLF is limited owing to strict feasibility conditions. Zheng et al. (2022b) proposed a scalable constraint technique based on a unified barrier function to transform a quadrotor control attitude system into an unconstrained dynamic system. While the technique can avoid the limitations of BLF, it does not take into account the velocity constraints. In the design process of the controller, the virtual control law inevitably needs to be derived. The dynamic surface control (DSC) technique is one of the commonly used methods to deal with this type of problem. However, in practice, DSC has two drawbacks. One is that

* Corresponding author.
E-mail addresses: lyy317040129@hrbeu.edu.cn (Y. Liu), xiaogong_lin@163.com (X. Lin), drliangkun@126.com (K. Liang).

https://doi.org/10.1016/j.oceaneng.2022.112710
Received 30 May 2022; Received in revised form 18 September 2022; Accepted 23 September 2022
Available online 14 October 2022

the virtual signal's differentiation increases the controller's computational burden. The second one is that DSC will result in unsmooth input and velocity-jump issue when a very strong transient force caused by the large initial position error is required to drive the DP ship to the desired position. Some scholars have already improved on the above limitations. One of the most popular methods is the bioinspired neurodynamics model. In Yang et al. (2011) and Wang et al. (2021), the bioinspired neurodynamics model was used to avoid the inherent complexity of numerical derivatives of virtual control signals and limited the output in a certain range in the backstepping design. Pan et al. (2015) solved the impractical velocity-jump issue by combining a bioinspired neurodynamics model in the backstepping tracking control of mobile robots. However, these works did not consider the dynamic safety constraints in tracking control. Thus, it is imperative to study the safety constraints including the position and velocity of the DP ship, while the proposed control law can easily be applied in application.

In the process of the tracking control design, it is necessary to consider the existence of model uncertainties and environmental disturbances, otherwise, these lumped disturbances seriously affect the trajectory tracking accuracy of the DP ship. Disturbance estimation methods based on neural networks and fuzzy logic systems can estimate the relevant disturbances rapidly, but have disadvantages such as heavy computational load, which increases the cost (Mu et al., 2018; Dang et al., 2022). Disturbance observer (DO) is an essential method to estimate the lumped disturbances formed by all uncertainties and disturbances of the DP ship and to reduce the control gain as a feedforward control (Sariyildiz et al., 2019). Besides DO can enhance the robustness, simplify observer structure and reduce computational effort simultaneously (Wei et al., 2022). Compared with the conventional DO, the sliding mode disturbance observer (SMDO) has the advantage of rapid convergence and robustness (Chen et al., 2017; Sun et al., 2018; Van, 2019). However, it is inevitable that the sliding mode control is terribly affected by chattering, and the chattering issue can negatively impact the normal operation of the DP ship (Sun et al., 2020). Hence, it is imperative to investigate this issue for the DP ship.

Motivated by the preceding researches, we propose a new robust tracking control method for the DP ship subject to model uncertainties, unknown environmental disturbances, and dynamic safety constraints. The key features are summarized as follows:

(a) A new robust tracking control framework is proposed based on UBF to ensure that the position and velocity of the DP ship are within the dynamic safety constraints.
(b) A bioinspired neurodynamics model is introduced to avoid complex differential calculation, simplify controller design, limit the virtual control in a certain range, and solve velocity-jump issue.
(c) To alleviate the chattering and have fast convergence performance, a practical SMDO is proposed in combination with the idea of boundary layers to estimate lumped disturbances including model uncertainties and unknown disturbances.

This paper is organized as follows. Section 2 introduces the model of the DP ship, some useful definitions, and lemmas. In Section 3, the robust tracking control framework with UBF, SMDO and BNDM is presented. In Section 4, simulation examples verify the effectiveness of the proposed method. The conclusion is drawn in Section 5.

2. Problem formulation

Notations: For any vector $\mu = [\mu_1, \dots, \mu_n]^T$ and any non-negative real number ϱ, we define $\lceil \mu^{\varrho} \rfloor \triangleq [|\mu_1|^{\varrho}\,\mathrm{sgn}(\mu_1), \cdots, |\mu_n|^{\varrho}\,\mathrm{sgn}(\mu_n)]^T$ and $\mathrm{sgn}(\mu) \triangleq [\mathrm{sgn}(\mu_1), \dots, \mathrm{sgn}(\mu_n)]^T$. $\|\cdot\|$ denotes the two-norm of a vector or a matrix. T_{ij} denotes the ith row and jth column of the matrix T. $I_{n\times n}$ denotes the identity matrix.

2.1. Mathematical model of the DP ship

The DP ship in our study is with fully actuated device. The mathematical model of the nonlinear motion of the DP ship is expressed as (Li and Lin, 2022) :

$$\begin{cases} \dot{\eta} = J(\psi)\upsilon \\ M\dot{\upsilon} + C(\upsilon)\upsilon + D(\upsilon)\upsilon = \tau + \tau_w \end{cases} \tag{1}$$

where $\eta = [x, y, \psi]^T \in \mathbb{R}^3$ is the position vector in the earth-fixed frame, consisting of the surge position x, the sway position y, and the heading $\psi \in [0, 2\pi]$ of the DP ship. $\upsilon = [u, v, r]^T \in \mathbb{R}^3$ is the velocity vector in the body-fixed frame, consisting of the surge velocity u, the sway velocity v, the yaw rate r of the DP ship. $J(\psi)$ is the rotation matrix expressed as

$$J(\psi) = \begin{bmatrix} \cos(\psi) & -\sin(\psi) & 0 \\ \sin(\psi) & \cos(\psi) & 0 \\ 0 & 0 & 1 \end{bmatrix} \tag{2}$$

with the property $\|J(\psi)\| = 1$. M is the inertial matrix including the added mass, which is invertible, symmetric and positive definite. $C(\upsilon)$ is the Coriolis and centripetal matrix; $D(\upsilon)$ is the damping matrix. These matrices are described as

$$M = \begin{bmatrix} m_{11} & 0 & 0 \\ 0 & m_{22} & m_{23} \\ 0 & m_{32} & m_{33} \end{bmatrix} \tag{3}$$

$$C(\upsilon) = \begin{bmatrix} 0 & 0 & -m_{22}v - m_{23}r \\ 0 & 0 & m_{11}u \\ m_{22}v + m_{23}r & -m_{11}u & 0 \end{bmatrix} \tag{4}$$

$$D(\upsilon) = \begin{bmatrix} d_{11} & 0 & 0 \\ 0 & d_{22} & d_{23} \\ 0 & d_{32} & d_{33} \end{bmatrix} \tag{5}$$

where $m_{11} = m - X_{\dot{u}}$, $m_{22} = m - Y_{\dot{v}}$, $m_{23} = m_{32} = mx_g - Y_{\dot{r}}$, $m_{33} = I_z - N_{\dot{r}}$, $d_{11} = -X_u - X_{|u|u}|u|$, $d_{22} = -Y_v - Y_{|v|v}|v| - Y_{|r|v}|r|$, $d_{23} = -Y_r - Y_{|v|r}|v| - Y_{|r|r}|r|$, $d_{32} = -N_v - N_{|v|v}|v| - N_{|r|v}|r|$, $d_{33} = -N_r - N_{|v|r}|v| - N_{|r|r}|r|$. Here, m is the mass of the DP ship, I_z is the moment of inertia about the earth-fixed frame, x_g is the distance from the origin of the body-fixed frame to the center of gravity of the ship. The other symbols X_*, Y_*, N_* are the corresponding hydrodynamic derivatives. $\tau = [\tau_1, \tau_2, \tau_3]^T \in \mathbb{R}^3$ is the control vector produced by the propulsion system, consisting of control forces τ_1 in surge and τ_2 in sway, and moment τ_3 in yaw. $\tau_w = [\tau_{w1}, \tau_{w2}, \tau_{w3}]^T \in \mathbb{R}^3$ is the environmental disturbance vector.

Assumption 1. The matrix M, $C(\upsilon)$ and $D(\upsilon)$ can be expressed as follows: $M = M_0 + M_\Delta$, $C(\upsilon) = C_0(\upsilon) + C_\Delta(\upsilon)$, $D(\upsilon) = D_0(\upsilon) + D_\Delta(\upsilon)$, where M_0, $C_0(\upsilon)$ and $D_0(\upsilon)$ are known matrices, M_Δ, $C_\Delta(\upsilon)$ and $D_\Delta(\upsilon)$ are unknown matrices (Qiao and Zhang, 2017, 2018, 2019).

Assumption 2. The disturbance $\tau_{wi} (i = 1, 2, 3)$ is unknown time-varying yet bounded.

Remark 1. The DP ship is characterized by high nonlinearity and strong coupling, and is inevitably influenced by environmental disturbances in the complex ocean. The effect of environmental disturbances and changes in navigation conditions leads to the parameter uncertainties of the hydrodynamic coefficients of the DP ship. Therefore, Assumption 1 is reasonable.

Remark 2. Since the ocean environment is constantly changing and has finite energy, the disturbances acting on the DP ship can be taken as unknown time-varying yet bounded signals with finite changing rates. Therefore, Assumption 2 is reasonable.

The Eq. (1) can be rewritten as follows:

$$\dot{\upsilon} = M_0^{-1}\left(-C_0(\upsilon)\upsilon - D_0(\upsilon)\upsilon + \tau\right) + \tau_d \tag{6}$$

where $\tau_d \in \mathbb{R}^3$ is the lumped disturbances including the environmental disturbances and model uncertainties, and can be described as follows:

$$\tau_d = M_0^{-1}\left(-M_\Delta\dot{\upsilon} - C_\Delta(\upsilon)\upsilon - D_\Delta(\upsilon)\upsilon + \tau_w\right) \tag{7}$$

Assumption 3. The lumped disturbances τ_d and derivative of τ_d are bounded, and exist unknown positive constants ι and $\bar{\iota}$ such that $\|\tau_d\| \le \iota$ and $\|\dot{\tau}_d\| \le \bar{\iota}$.

2.2. Definitions and lemmas

Definition 1. A scalar function f of the variable x on an open region $\aleph$ is a unified barrier function (UBF) and constructed as Zhao et al. (2020)

$$f = \frac{x - \overline{\alpha}_l}{x - \alpha_l(t)} - \frac{x - \underline{\alpha}_h}{x - \alpha_h(t)} \tag{8}$$

where the initial state satisfying $x(0) \in \aleph$, $\overline{\alpha}_l$ is the upper bound of $\alpha_l(t)$ satisfies $\alpha_l(t) < \overline{\alpha}_l$, $\underline{\alpha}_h$ is the lower bound of $\alpha_h(t)$ satisfies $\underline{\alpha}_h < \alpha_h(t)$. From (8), we can clearly see that f exhibits two properties: (1) $f \to -\infty$ if $x \to \alpha_l^+(t)$; (2) $f \to +\infty$ if $x \to \alpha_h^-(t)$. Hence, it can be used to deal with the time-varying yet asymmetric constraints without changing the function structure.

Definition 2. The bioinspired neurodynamic model is defined as follows: (Wang et al., 2021)

$$\frac{d\xi_i}{dt} = (A - \xi_i)\phi(x) - B\xi_i - (P + \xi_i)g(x) \tag{9}$$

where ξ_i is the neural activity of ith neuron in the neural network; A and P are the upper and lower bounds of the neural activity respectively; B is the passive decay rate; $\phi(x)$ and $g(x)$ represent the excitatory and inhibitory inputs, and are defined as follows:

$$\phi(x) = \begin{cases} x, & x \ge 0 \\ 0, & x < 0, \end{cases} \quad g(x) = \begin{cases} -x, & x \le 0 \\ 0, & x > 0. \end{cases} \tag{10}$$

Lemma 1 (*Schur complement lemma*). *Let the partitioned matrix*

$$B = \begin{bmatrix} B_{11} & B_{12} \\ B_{21} & B_{22} \end{bmatrix} \tag{11}$$

by symmetric. Then,

$$\begin{aligned} B < 0 &\iff B_{11} < 0, S_{cb}(B_{11}) < 0 \\ &\iff B_{22} < 0, S_{cb}(B_{22}) < 0 \end{aligned} \tag{12}$$

or

$$\begin{aligned} B > 0 &\iff B_{11} > 0, S_{cb}(B_{11}) > 0 \\ &\iff B_{22} > 0, S_{cb}(B_{22}) > 0 \end{aligned} \tag{13}$$

where $S_{cb}(B_{11}) = B_{22} - B_{21}B_{11}^{-1}B_{12}$ *and* $S_{cb}(B_{22}) = B_{11} - B_{12}B_{22}^{-1}B_{21}$.

3. Robust tracking control design

3.1. Sliding mode disturbance observer

In this subsection, we construct a SMDO to estimate the lumped disturbances. Inspired by Sun et al. (2020), the SMDO is designed as follows:

$$\begin{aligned} \dot{\hat{\upsilon}} =& M_0^{-1}\left(-C_0(\upsilon)\upsilon - D_0(\upsilon)\upsilon + \tau\right) + \rho_1 \lceil e_o \rfloor^{\frac{1}{2}} \\ &+ \rho_2 e_o + k_o\beta \end{aligned} \tag{14}$$

$$\dot{\beta} = \rho_3\,\mathrm{sgn}(e_o) + \rho_4 e_o - \rho_5\beta \tag{15}$$

$$\hat{\tau}_d = k_o\beta \tag{16}$$

where $\beta \in \mathbb{R}^3$; $\rho_j = \mathrm{diag}([\rho_{j1}, \rho_{j2}, \rho_{j3}]^T)$, $k_o = \mathrm{diag}([k_{o1}, k_{o2}, k_{o3}]^T)$, ρ_{ji} and k_{oi} are positive design parameters for $j = 1,2,3,4,5$ and $i = 1,2,3$; $\hat{\upsilon}$ and $\hat{\tau}_d$ are the velocity estimation of υ and the disturbance estimation of τ_d, respectively; $e_o = [e_{o1}, e_{o2}, e_{o3}]^T$ is the velocity estimation error and $e_o = \upsilon - \hat{\upsilon}$; $\tilde{\tau}_d = \tau_d - \hat{\tau}_d$ is the observer error.

Remark 3. The advantage of the SMDO in (14)–(16) is that it can effectively estimate the lumped disturbances of the DP ship by embedding an improved super-twisting algorithm. $\mathrm{sgn}(e_o)$ is used to guarantee the stability of sliding-mode-based algorithms. In practical application, the chattering is inevitable due to the switching delay. To make SMDO have less chattering, the continuous saturation function was used to approximate $\mathrm{sgn}(e_o)$ (Riani et al., 2018):

$$\mathrm{sat}(e_o, \epsilon) = \begin{cases} \mathrm{sgn}(e_o), & |e_o| \ge \epsilon \\ \frac{e_o}{\epsilon}, & \text{else} \end{cases} \tag{17}$$

where ϵ denotes the width of boundary layer and satisfies $\epsilon > 0$. Significantly, ϵ is a really small constant.

Theorem 1. *Consider the DP ship (1) under the lumped disturbances (7), SMDO (14)–(16) and Assumption 3. The observer error* $\tilde{\tau}_d$ *exponentially converges to zero by selecting the design parameters* ρ_{ji} *and* k_{oi} *satisfy (26).*

Proof. We use the above equation and (14) to obtain the time derivative of the velocity estimation error e_o as

$$\dot{e}_o = \tilde{\tau}_d - \rho_1 \lceil e_o \rfloor^{\frac{1}{2}} - \rho_2 e_o \tag{18}$$

The time derivative of the observer error $\tilde{\tau}_d$ along (15) and (16) is

$$\begin{aligned} \dot{\tilde{\tau}}_d =& \dot{\tau}_d - k_o\rho_3\,\mathrm{sgn}(e_o) - k_o\rho_4 e_o + \rho_5\hat{\tau}_d \\ =& -\overline{\rho}_3\,\mathrm{sgn}(e_o) - \overline{\rho}_4 e_o - \rho_5\tilde{\tau}_d + \dot{\tau}_d + \rho_5\tau_d \end{aligned} \tag{19}$$

where $\overline{\rho}_3 \triangleq k_o\rho_3$, $\overline{\rho}_4 \triangleq k_o\rho_4$. Consider the candidate Lyapunov function $V = \sum_{i=1}^3 V_i$, V_i is as follows:

$$\begin{aligned} V_i =& \frac{1}{2}\left(\rho_{1i}|e_{oi}|^{\frac{1}{2}}\,\mathrm{sgn}(e_{oi}) + \rho_{2i}e_{oi} - \tilde{\tau}_{di}\right)^2 + \frac{1}{2}\tilde{\tau}_{di}^2 \\ &+ 2\overline{\rho}_{3i}|e_{oi}| + \overline{\rho}_{4i}e_{oi}^2 \end{aligned} \tag{20}$$

where e_{oi} and $\tilde{\tau}_{di}$ are the ith element of e_o and $\tilde{\tau}_d$, respectively; $\overline{\rho}_{3i}$ is the ith element on the primary diagonal of $\overline{\rho}_3$. Note that the following inequality always holds:

$$\underline{\delta}_i\|\hbar_i\|^2 \le V_i \le \overline{\delta}_i\|\hbar_i\|^2 \tag{21}$$

with positive constants $\underline{\delta}_i$ and $\overline{\delta}_i$, and $\hbar_i = [\lceil e_{oi}^{\frac{1}{2}} \rfloor, e_{oi}, \tilde{\tau}_{di}]^T$.

The time derivative of V_i is as follows:

$$\begin{aligned} \dot{V}_i =& \rho_{1i}|e_{oi}|^{\frac{1}{2}}\,\mathrm{sgn}(e_{oi})\left(\frac{1}{2}\rho_{1i}|e_{oi}|^{-\frac{1}{2}}\dot{e}_{oi} + \rho_{2i}\dot{e}_{oi} - \dot{\tilde{\tau}}_{di}\right) \\ &+ \rho_{2i}e_{oi}\left(\frac{1}{2}\rho_{1i}|e_{oi}|^{-\frac{1}{2}}\dot{e}_{oi} + \rho_{2i}\dot{e}_{oi} - \dot{\tilde{\tau}}_{di}\right) \\ &- \dot{\tilde{\tau}}_{di}\left(\frac{1}{2}\rho_{1i}|e_{oi}|^{-\frac{1}{2}}\dot{e}_{oi} + \rho_{2i}\dot{e}_{oi} - \dot{\tilde{\tau}}_{di}\right) \\ &+ 2\overline{\rho}_{3i}\dot{e}_{oi}\,\mathrm{sgn}(e_{oi}) + 2\overline{\rho}_{4i}e_{oi}\dot{e}_{oi} + \tilde{\tau}_{di}\dot{\tau}_{di} \\ =& \Delta_1 + \Delta_2 + \Delta_3 + \Delta_4 \\ =& \left(2\tilde{\tau}_{di} - \rho_{1i}|e_{oi}|^{\frac{1}{2}}\,\mathrm{sgn}(e_{oi}) - \rho_{2i}e_{oi}\right)(\dot{\tau}_{di} + \rho_{5i}\tau_{di}) \\ &- \frac{1}{|e_{oi}|^{\frac{1}{2}}}\hbar_i^T\mathrm{N}_i^1\hbar_i - \hbar_i^T\mathrm{N}_i^2\hbar_i \end{aligned} \tag{22}$$

where

$$\begin{aligned}
\Delta_1 =&\rho_{1i}|e_{oi}|^{\frac{1}{2}}\operatorname{sgn}(e_{oi})\left(\frac{1}{2}\rho_{1i}|e_{oi}|^{-\frac{1}{2}}\dot{e}_{oi}+\rho_{2i}\dot{e}_{oi}-\dot{\tilde{\tau}}_{di}\right)\\
=&\rho_{1i}\rho_{2i}\tilde{\tau}_{di}|e_{oi}|^{\frac{1}{2}}\operatorname{sgn}(e_{oi})-\rho_{1i}\rho_{2i}^2|e_{oi}|^{\frac{3}{2}}+\rho_{1i}\bar{\rho}_{3i}|e_{oi}|^{\frac{1}{2}}\\
&+\frac{1}{2}\rho_{1i}^2\tilde{\tau}_{di}\operatorname{sgn}(e_{oi})-\frac{1}{2}\rho_{1i}^3|e_{oi}|^{\frac{1}{2}}-\frac{3}{2}\rho_{1i}^2\rho_{2i}|e_{oi}|\\
&+\rho_{1i}\rho_{5i}\tilde{\tau}_{di}|e_{oi}|^{\frac{1}{2}}\operatorname{sgn}(e_{oi})+\rho_{1i}\bar{\rho}_{4i}|e_{oi}|^{\frac{3}{2}}\\
&-\rho_{1i}|e_{oi}|^{\frac{1}{2}}\operatorname{sgn}(e_{oi})\left(\dot{\tau}_{di}+\rho_{5i}\tau_{di}\right)\\
\Delta_2 =&\rho_{2i}e_{oi}\left(\frac{1}{2}\rho_{1i}|e_{oi}|^{-\frac{1}{2}}\dot{e}_{oi}+\rho_{2i}\dot{e}_{oi}-\dot{\tilde{\tau}}_{di}\right)\\
=&\frac{1}{2}\rho_{1i}\rho_{2i}\tilde{\tau}_{di}|e_{oi}|^{\frac{1}{2}}\operatorname{sgn}(e_{oi})-\frac{1}{2}\rho_{1i}^2\rho_{2i}|e_{oi}|-\rho_{2i}^3e_{oi}^2\\
&+\rho_{2i}^2\tilde{\tau}_{di}|e_{oi}|\operatorname{sgn}(e_{oi})+\rho_{2i}\bar{\rho}_{3i}|e_{oi}|-\frac{3}{2}\rho_{1i}\rho_{2i}^2|e_{oi}|^{\frac{3}{2}}\\
&+\rho_{2i}\rho_{5i}\tilde{\tau}_{di}|e_{oi}|\operatorname{sgn}(e_{oi})+\rho_{2i}\bar{\rho}_{4i}e_{oi}^2\\
&-\rho_{2i}|e_{oi}|\operatorname{sgn}(e_{oi})\left(\dot{\tau}_{di}+\rho_{5i}\tau_{di}\right)\\
\Delta_3 =&-\dot{\tilde{\tau}}_{di}\left(\frac{1}{2}\rho_{1i}|e_{oi}|^{-\frac{1}{2}}\dot{e}_{oi}+\rho_{2i}\dot{e}_{oi}-\dot{\tilde{\tau}}_{di}\right)\\
=&-\frac{1}{2}\rho_{1i}|e_{oi}|^{-\frac{1}{2}}\tilde{\tau}_{di}^2+\frac{1}{2}\rho_{1i}^2\operatorname{sgn}(e_{oi})\tilde{\tau}_{di}-\bar{\rho}_{3i}\operatorname{sgn}(e_{oi})\tilde{\tau}_{di}\\
&-\rho_{2i}\tilde{\tau}_{di}^2+\rho_{2i}^2e_{oi}\tilde{\tau}_{di}+\frac{3}{2}\rho_{1i}\rho_{2i}|e_{oi}|^{\frac{1}{2}}\operatorname{sgn}(e_{oi})\tilde{\tau}_{di}\\
&-\rho_{5i}\tilde{\tau}_{di}^2-\bar{\rho}_{4i}e_{oi}\tilde{\tau}_{di}+\tilde{\tau}_{di}\left(\dot{\tau}_{di}+\rho_{5i}\tau_{di}\right)\\
\Delta_4 =&2\bar{\rho}_{3i}\dot{e}_{oi}\operatorname{sgn}(e_{oi})+2\bar{\rho}_{4i}e_{oi}\dot{e}_{oi}+\tilde{\tau}_{di}\dot{\tau}_{di}\\
=&-2\rho_{1i}\bar{\rho}_{3i}|e_{o1}|^{\frac{1}{2}}-2\rho_{2i}\bar{\rho}_{3i}|e_{oi}|+\bar{\rho}_{3i}\tilde{\tau}_{di}-4\bar{\rho}_{4i}\tilde{\tau}_{di}e_{oi}\\
&-\rho_{5i}\tilde{\tau}_{di}^2+2\bar{\rho}_{4i}e_{oi}\tilde{\tau}_{di}-2\rho_{1i}\bar{\rho}_{4i}|e_{oi}|^{\frac{3}{2}}-2\rho_{2i}\bar{\rho}_{4i}e_{oi}^2\\
&+\tilde{\tau}_{di}\left(\dot{\tau}_{di}+\rho_{5i}\tau_{di}\right)
\end{aligned}$$

$$\mathrm{N}_i^1=\begin{bmatrix}\frac{\rho_{1i}(\rho_{1i}^2+2\bar{\rho}_{3i})}{2} & 0 & \frac{-\rho_{1i}^2}{2}\\ 0 & \frac{\rho_{1i}(5\rho_{2i}^2+2\bar{\rho}_{4i})}{2} & \frac{-3\rho_{1i}\rho_{2i}}{2}\\ \frac{-\rho_{1i}^2}{2} & \frac{-3\rho_{1i}\rho_{2i}}{2} & \frac{\rho_{1i}}{2}\end{bmatrix}$$

$$\mathrm{N}_i^2=\begin{bmatrix}\rho_{2i}(\bar{\rho}_{3i}+2\rho_{1i}^2) & 0 & -\frac{\rho_{1i}\rho_{5i}}{2}\\ 0 & \rho_{2i}(\rho_{2i}^2+\bar{\rho}_{4i}) & -\frac{\rho_{2i}(2\rho_{2i}+\rho_{5i})}{2}\\ -\frac{\rho_{1i}\rho_{5i}}{2} & -\frac{\rho_{2i}(2\rho_{2i}+\rho_{5i})}{2} & \rho_{2i}+2\rho_{5i}\end{bmatrix}$$

Since Assumption 3 holds, we get $\dot{\tau}_{di}+\rho_{5i}\tau_{di}\le\ell_i$. Thus, from (22), we have

$$\begin{aligned}
\dot{V}_i\le&\ell_i\left(2\tilde{\tau}_{di}+\rho_{1i}|e_{oi}|^{\frac{1}{2}}\operatorname{sgn}(e_{oi})+\rho_{2i}e_{oi}\right)\\
&-\frac{1}{|e_{oi}|^{\frac{1}{2}}}\hbar_i^T\mathrm{N}_i^1\hbar_i-\hbar_i^T\mathrm{N}_i^2\hbar_i
\end{aligned}\tag{23}$$

Now Young's inequality can be employed to obtain

$$\begin{cases}2\ell_i\tilde{\tau}_{di}\le\frac{1}{2}+2\ell_i^2\tilde{\tau}_{di}^2\\ \ell_i\rho_{2i}e_{oi}\le\frac{1}{2}+\frac{\ell_i^2\rho_{2i}^2e_{oi}^2}{2}\\ \ell_i\rho_{1i}|e_{oi}|^{\frac{1}{2}}\operatorname{sgn}(e_{oi})\le\frac{1}{2}+\frac{\ell_i^2\rho_{1i}^2|e_{oi}|}{2}\end{cases}\tag{24}$$

We use the above equation and (24) to rewrite (23) as

$$\dot{V}_i\le-\frac{1}{|e_{oi}|^{\frac{1}{2}}}\hbar_i^T\mathrm{N}_i^1\hbar_i-\hbar_i^T\overline{\mathrm{N}}_i^2\hbar_i+\mathrm{C}\tag{25}$$

where $\overline{\mathrm{N}}_i^2\in\mathbb{R}^3$ with matrix elements $\overline{\mathrm{N}}_{i11}^2=\rho_{2i}(\bar{\rho}_{3i}+2\rho_{2i}^2)-\ell_i^2\rho_{1i}^2/2$, $\overline{\mathrm{N}}_{i22}^2=\rho_{2i}(\rho_{2i}^2+\bar{\rho}_{4i})-\ell_i^2\rho_{2i}^2/2$, $\overline{\mathrm{N}}_{i33}^2=\rho_{2i}+2\rho_{5i}-2\ell_i^2$, $\overline{\mathrm{N}}_{i12}^2=\overline{\mathrm{N}}_{i21}^2=0$, $\overline{\mathrm{N}}_{i13}^2=\overline{\mathrm{N}}_{i31}^2=-\rho_{1i}\rho_{5i}/2$, $\overline{\mathrm{N}}_{i23}^2=\overline{\mathrm{N}}_{i32}^2=-\rho_{2i}(\rho_{2i}+\rho_{5i})/2$, and C is a constant.

According Lemma 1, to ensure the matrices N_i^1 and $\overline{\mathrm{N}}_i^2$ are positive-definite, the designed parameters ρ_{1i}, ρ_{2i}, $\bar{\rho}_{3i}$, $\bar{\rho}_{4i}$, ρ_{5i} satisfy

$$\begin{cases}\rho_{4i}^4+\rho_{2i}^2\rho_{5i}^2+3\bar{\rho}_{3i}\rho_{2i}^2-6\rho_{2i}\bar{\rho}_{3i}\rho_{5i}-2\rho_{1i}^2\rho_{2i}\rho_{5i}\\ -2\bar{\rho}_{3i}\bar{\rho}_{4i}-2\rho_{2i}^3\bar{\rho}_{3i}>0\\ \rho_{2i}\bar{\rho}_{4i}\rho_{5i}+3\rho_{2i}^2\bar{\rho}_{4i}+3\rho_{2i}^3\rho_{5i}+\ell_i^4\rho_{2i}^2-\ell_i^2\rho_{2i}^2\rho_{5i}\\ -2\ell_i^2\rho_{2i}\bar{\rho}_{4i}-\bar{\rho}_{4i}^2-5\ell_i^2\rho_{2i}^3/2-\rho_{2i}^2\rho_{5i}^2/4>0\\ \ell_i^2\rho_{1i}^2/2-3\rho_{2i}\rho_{3i}-2\rho_{1i}^2\rho_{2i}>0\end{cases}\tag{26}$$

Thus, (25) can be used to obtain

$$\dot{V}_i\le-\hbar_i^T\overline{\mathrm{N}}_i^2\hbar_i\le-\lambda_{\min}(\overline{\mathrm{N}}_i^2)\|\hbar_i\|^2\tag{27}$$

with $\lambda_{\min}(\overline{\mathrm{N}}_i^2)>0$. Obviously, V satisfies $\sum_{i=1}^3\underline{\delta}_i\|\hbar_i\|^2\le\sum_{i=1}^3V_i\le\sum_{i=1}^3\bar{\delta}_i\|\hbar_i\|^2$ and $\dot{V}\le-\sum_{i=1}^3\lambda_{\min}(\overline{\mathrm{N}}_i^2)\|\hbar_i\|^2$. From Theorem 1, the proposed observer is stable and its estimation converges to the lumped disturbances. □

3.2. Tracking control design

In this subsection, we design a UBF-based robust tracking controller for the DP ship that combines the disturbance observer (14) and bioinspired neurodynamics model to track the desired trajectory and keep the position and velocity within the set of the predefined constraint. The design process consists of the following steps:

Step 1: Transform the position of the DP ship using the UBF as

$$f_\eta=\frac{\eta-\bar{a}_l}{\eta-a_l(t)}-\frac{\eta-\underline{a}_h}{\eta-a_h(t)}\tag{28}$$

Rewrite the preceding equation as

$$f_\eta=\Theta_1\eta+\Theta_2\tag{29}$$

with $\Theta_1=\operatorname{diag}([\Theta_{11},\Theta_{12},\Theta_{13}]^T)$, $\Theta_{1i}=\frac{\bar{a}_{li}-a_{li}+a_{hi}-\underline{a}_{hi}}{(\eta_i-a_{li})(a_{hi}-\eta_i)}$, $\Theta_2=[\Theta_{21},\Theta_{22},\Theta_{23}]^T$, $\Theta_{2i}=\frac{a_{li}\underline{a}_{hi}-\bar{a}_{li}a_{hi}}{(\eta_i-a_{li})(a_{hi}-\eta_i)}$. The time derivative of f_η is as follows:

$$\dot{f}_\eta=\overline{\Theta}_1\dot{\eta}+\overline{\Theta}_2\tag{30}$$

with $\overline{\Theta}_1=\operatorname{diag}([\overline{\Theta}_{11},\overline{\Theta}_{12},\overline{\Theta}_{13}]^T)$, $\overline{\Theta}_{1i}=\frac{\bar{a}_{li}-a_{li}}{(\eta_i-a_{li})^2}+\frac{a_{hi}-\underline{a}_{hi}}{(\eta_i-a_{hi})^2}$, $\overline{\Theta}_2=[\overline{\Theta}_{21},\overline{\Theta}_{22},\overline{\Theta}_{23}]^T$, $\overline{\Theta}_{2i}=\frac{(\eta_i-\bar{a}_{li})\dot{a}_{li}}{(\eta_i-a_{li})^2}-\frac{(\eta_i-\underline{a}_{hi})\dot{a}_{hi}}{(\eta_i-a_{hi})^2}$.

Transform the velocity of the DP ship using the UBF as

$$f_\upsilon=\frac{\upsilon-\bar{b}_l}{\upsilon-b_l(t)}-\frac{\upsilon-\underline{b}_h}{\upsilon-b_h(t)}\tag{31}$$

Rewrite the preceding equation as

$$f_\upsilon=\Lambda_1\upsilon+\Lambda_2\tag{32}$$

with $\Lambda_1=\operatorname{diag}([\Lambda_{11},\Lambda_{12},\Lambda_{13}]^T)$, $\Lambda_{1i}=\frac{\bar{b}_{li}-b_{li}+b_{hi}-\underline{b}_{hi}}{(\upsilon_i-b_{li})(b_{hi}-\upsilon_i)}$, $\Lambda_2=[\Lambda_{21},\Lambda_{22},\Lambda_{23}]^T$, $\Lambda_{2i}=\frac{b_{li}\underline{b}_{hi}-\bar{b}_{li}b_{hi}}{(\upsilon_i-b_{li})(b_{hi}-\upsilon_i)}$. The time derivative of f_υ is as follows:

$$\dot{f}_\upsilon=\overline{\Lambda}_1\dot{\upsilon}+\overline{\Lambda}_2\tag{33}$$

with $\overline{\Lambda}_1=\operatorname{diag}([\overline{\Lambda}_{11},\overline{\Lambda}_{12},\overline{\Lambda}_{13}]^T)$, $\overline{\Lambda}_{1i}=\frac{\bar{b}_{li}-b_{li}}{(\upsilon_i-b_{li})^2}+\frac{b_{hi}-\underline{b}_{hi}}{(\upsilon_i-b_{hi})^2}$, $\overline{\Lambda}_2=[\overline{\Lambda}_{21},\overline{\Lambda}_{22},\overline{\Lambda}_{23}]^T$, $\overline{\Lambda}_{2i}=\frac{(\upsilon_i-\bar{b}_{li})\dot{b}_{li}}{(\upsilon_i-b_{li})^2}-\frac{(\upsilon_i-\underline{b}_{hi})\dot{b}_{hi}}{(\upsilon_i-b_{hi})^2}$.

Step 2: Define the tracking error as

$$e_\eta=f_\eta-f_{\eta_d}\tag{34}$$

where $f_{\eta_d}=\frac{\eta_d-\bar{a}_l}{\eta_d-a_l(t)}-\frac{\eta_d-\underline{a}_h}{\eta_d-a_h(t)}$. The time derivative of e_η is as follows

$$\dot{e}_\eta=\overline{\Theta}_1J(\psi)\Lambda_1^{-1}f_\upsilon-\overline{\Theta}_1J(\psi)\Lambda_1^{-1}\Lambda_2+\overline{\Theta}_2-\dot{f}_{\eta_d}\tag{35}$$

Choose the virtual control law z_υ as

$$z_\upsilon=\Lambda_1J(\psi)^T\overline{\Theta}_1^{-1}(-K_1e_\eta-\overline{\Theta}_2+\dot{f}_{\eta_d})+\Lambda_2\tag{36}$$

with $K_1\in\mathbb{R}^{3\times3}$ is the design matrix.

Step 3: To avoid differential exploration and simplify control design, a bioinspired neurodynamics model was introduced in Definition 2. Let the virtual control vector $z_\upsilon \in \mathbb{R}^3$ go through the bioinspired neurodynamics model. Then, we have

$$\dot{\bar{z}}_\upsilon = \begin{bmatrix} (A_1 - \bar{z}_{\upsilon 1})\phi(z_{\upsilon 1}) - B_1\bar{z}_{\upsilon 1} - (P_1 + \bar{z}_{\upsilon 1})g(z_{\upsilon 1}) \\ (A_2 - \bar{z}_{\upsilon 2})\phi(z_{\upsilon 2}) - B_2\bar{z}_{\upsilon 2} - (P_2 + \bar{z}_{\upsilon 2})g(z_{\upsilon 2}) \\ (A_3 - \bar{z}_{\upsilon 3})\phi(z_{\upsilon 3}) - B_3\bar{z}_{\upsilon 3} - (P_3 + \bar{z}_{\upsilon 3})g(z_{\upsilon 3}) \end{bmatrix} \tag{37}$$

where A_i, B_i and P_i $(i = 1, 2, 3)$ are design parameters, respectively; $\phi(z_{\upsilon i})$ and $g(z_{\upsilon i})$ satisfy

$$\phi(z_{\upsilon i}) = \begin{cases} z_{\upsilon i}, & z_{\upsilon i} \geq 0 \\ 0, & z_{\upsilon i} < 0, \end{cases} \quad g(z_{\upsilon i}) = \begin{cases} -z_{\upsilon i}, & z_{\upsilon i} \leq 0 \\ 0, & z_{\upsilon i} > 0 \end{cases} \tag{38}$$

Step 4: Define the velocity error as

$$e_\upsilon = f_\upsilon - \bar{z}_\upsilon \tag{39}$$

The time derivative of e_υ is as follows:

$$\dot{e}_\upsilon = \overline{\Lambda}_1 \left(M_0^{-1}(-C_0(\upsilon)\upsilon - D_0(\upsilon)\upsilon + \tau) + \tau_d \right) + \overline{\Lambda}_2 - \dot{\bar{z}}_\upsilon \tag{40}$$

We propose a tracking control law as follows:

$$\begin{aligned} \tau =& M_0\overline{\Lambda}_1^{-1}\left(-K_2 e_\upsilon - \overline{\Lambda}_2 + \dot{\bar{z}}_\upsilon - \Lambda_1^{-1}J(\psi)^T\overline{\Theta}_1 e_\eta\right) \\ &+ C_0(\upsilon)\upsilon + D_0(\upsilon)\upsilon - M_0\hat{\tau}_d \end{aligned} \tag{41}$$

with $K_2 \in \mathbb{R}^{3\times 3}$ is the design matrix.

Theorem 2. *Consider the DP ship (1) under the lumped disturbances (7) and dynamic safety constraints (a_l, a_h, b_l, b_h), the tracking controller including the UBF constructions (28) and (31), virtual control law (36), BNDM (37) and SMDO (14)–(16) guarantees that: (1) all signals in the DP closed-loop control system are bounded; (2) the position and velocity of the DP ship are within the dynamic safety constraints by properly selecting K_1, K_2, A_i, B_i and P_i; and (3) the true tracking error is bounded.*

Proof. Consider the candidate Lyapunov function as

$$V_4 = \frac{1}{2}e_\eta^T e_\eta + \frac{1}{2}e_\upsilon^T e_\upsilon + \frac{1}{2}e_z^T e_z \tag{42}$$

where $e_z \in \mathbb{R}^3$ is defined as

$$e_z = \bar{z}_\upsilon - z_\upsilon. \tag{43}$$

Therefore, the derivative of (42) can be obtained using (35), (40) and the above equation as follows:

$$\begin{aligned} \dot{V}_4 =& -e_\eta^T K_1 e_\eta - e_\upsilon^T K_2 e_\upsilon + e_\upsilon^T\overline{\Lambda}_1\tilde{\tau}_d + e_z^T\dot{e}_z \\ &+ e_\eta^T\overline{\Theta}_1 J(\psi)\Lambda_1^{-1}e_z \end{aligned} \tag{44}$$

Using Young's inequality, we can obtain

$$\begin{cases} e_\upsilon^T\overline{\Lambda}_1\tilde{\tau}_d \leq \frac{1}{2}e_\upsilon^T\overline{\Lambda}_1^2 e_\upsilon + \frac{1}{2}\tilde{\tau}_d^T\tilde{\tau}_d \\ e_\eta^T\overline{\Theta}_1 J(\psi)\Lambda_1^{-1}e_z \leq \frac{1}{2}e_\eta^T\overline{\Theta}_1^2 e_\eta + \frac{1}{2}e_z^T\Lambda_1^{-2}e_z \end{cases} \tag{45}$$

Substituting (45) into (44) results in

$$\begin{aligned} \dot{V}_4 \leq& -e_\eta^T\left(K_1 - \frac{1}{2}\overline{\Theta}_1^2\right)e_\eta - e_\upsilon^T\left(K_2 - \frac{1}{2}\overline{\Lambda}_1^2\right)e_\upsilon \\ &+ \frac{1}{2}e_z^T\Lambda_1^{-2}e_z + e_z^T\dot{e}_z + \frac{1}{2}\tilde{\tau}_d^T\tilde{\tau}_d \end{aligned} \tag{46}$$

As it can be seen from (42) and (46), it is required to calculate e_z and $\dot{e}_z$. Rewrite ith row of (37) as

$$\dot{\bar{z}}_{\upsilon i} = -\left(B_i + \phi(z_{\upsilon i}) + g(z_{\upsilon i})\right)\bar{z}_{\upsilon i} + A_i\phi(z_{\upsilon i}) - P_i g(z_{\upsilon i}) \tag{47}$$

Let $B_i + \phi(z_{\upsilon i}) + g(z_{\upsilon i}) = H_i$, $A_i = P_i$. Then, the time derivative of ith element of e_z is as follows:

$$\dot{e}_{zi} = -H_i\bar{z}_{\upsilon i} + A_i z_{\upsilon i} - \dot{z}_{\upsilon i} \tag{48}$$

Let $A_i = H_i$, substituting (48) into (46) yields

$$\begin{aligned} \dot{V}_4 \leq& -e_\eta^T\left(K_1 - \frac{1}{2}\overline{\Theta}_1^2\right)e_\eta - e_\upsilon^T\left(K_2 - \frac{1}{2}\overline{\Lambda}_1^2\right)e_\upsilon \\ &- e_z^T\left(H - \frac{1}{2}\Lambda_1^{-2}\right)e_z + e_z^T\dot{z}_\upsilon + \frac{1}{2}\tilde{\tau}_d^T\tilde{\tau}_d \end{aligned} \tag{49}$$

where $H = \mathrm{diag}([H_1, H_2, H_3]^T)$. According to Young's inequality, we have

$$e_z^T\dot{z}_\upsilon \leq \frac{1}{2}e_z^T e_z + \frac{1}{2}\dot{z}_\upsilon^T\dot{z}_\upsilon \tag{50}$$

Substituting (50) into (49) results in

$$\dot{V}_4 \leq -e_\eta^T\Xi_1 e_\eta - e_\upsilon^T\Xi_2 e_\upsilon - e_z^T\Xi_3 e_z + \Xi_4 \tag{51}$$

where $\Xi_1 = K_1 - \frac{1}{2}\overline{\Theta}_1^2$, $\Xi_2 = K_2 - \frac{1}{2}\overline{\Lambda}_1^2$, $\Xi_3 = H - \frac{1}{2}\Lambda_1^{-2} - \frac{1}{2}I_{3\times 3}$ and $\Xi_4 = \frac{1}{2}\dot{z}_\upsilon^T\dot{z}_\upsilon + \frac{1}{2}\tilde{\tau}_d^T\tilde{\tau}_d$. In order to guarantee the stability of the DP ship, let $\lambda_{\min}(\Xi_1) > 0$, $\lambda_{\min}(\Xi_2) > 0$ and $\lambda_{\min}(\Xi_3) > 0$. From the perspective of practical application, the control input and velocity of the DP ship are all bounded. $\dot{z}_\upsilon$ is a continuous and bounded function. The observer error $\tilde{\tau}_d$ is bounded from Theorem 1. Hence, Ξ_4 is bounded. By defining $\underline{\Xi} = \min\left\{\lambda_{\min}(\Xi_1), \lambda_{\min}(\Xi_2), \lambda_{\min}(\Xi_3)\right\}$, we have

$$\dot{V}_4 \leq -2\underline{\Xi}V + \Xi_4 \tag{52}$$

By solving the proceeding equation, we have

$$0 \leq V_4(t) \leq \frac{\Xi_4}{2\underline{\Xi}} + \left(V_4(0) - \frac{\Xi_4}{2\underline{\Xi}}\right)e^{-2\underline{\Xi}t} \tag{53}$$

It is obviously seen that $V_4(t)$ is uniformly ultimately bounded. From (28), (31) and (42), we know that e_η, e_υ and e_z are bounded and the position and velocity of the DP ship can be strictly confined in the dynamic safety constraints.

Furthermore, we need to show that the true tracking error is bounded. Define the true tracking error e_t as

$$e_t = \eta - \eta_d \tag{54}$$

From (28), the relationship between e_t and e_η is as follows:

$$e_t = \Gamma^{-1}e_\eta \tag{55}$$

where $\Gamma = \mathrm{diag}t([\Gamma_1, \Gamma_2, \Gamma_3]^T)$ and $\Gamma_i = \frac{\bar{a}_{li} - a_{li}}{(\eta_i - a_{li})(\eta_{di} - a_{li})} + \frac{a_{hi} - a_{hi}}{(a_{hi} - \eta_i)(a_{hi} - \eta_{di})}$.

From Definition 1, we know that η_i is within the subset $\aleph_\eta$ and $\eta_{di} \in \aleph_{\eta_d} \subset \aleph_\eta$. One has to show that there exist positive constants $\overline{\kappa}_{in}$ and $\underline{\kappa}_{in}$ $(i = 1, 2, 3; n = 1, 2)$ such that

$$\begin{cases} 0 \leq \underline{\kappa}_{i1} \leq (\eta_i - a_{li})(\eta_{di} - a_{li}) \leq \overline{\kappa}_{i1} \\ 0 \leq \underline{\kappa}_{i2} \leq (a_{hi} - \eta_i)(a_{hi} - \eta_{di}) \leq \overline{\kappa}_{i2} \end{cases} \tag{56}$$

From (56), it can be seen that there exist constants $\overline{\Gamma}_i$ and $\underline{\Gamma}_i$ such that

$$0 \leq \underline{\Gamma}_i \leq \Gamma_i \leq \overline{\Gamma}_i \tag{57}$$

As a result, the true tracking error is bounded. □

4. Simulations

In this section, simulations show the effectiveness of the proposed observer and tracking controller for the DP ship. The ship model used in this paper is Cybership-II and the above parameters are in Table 1 (Skjetne et al., 2005). To explore the effectiveness of the proposed observer and controller, two control methods were chosen for comparison. The first one is the traditional backstepping (BS) method without UBF. The second one is the method in Li et al. (2022a). .

The desired trajectory is selected as: (a) $t \leq 10$, $\eta_d = [0.1t^2 - 10, -10, 0]^T$; (b) $t > 10$, $\eta_d = [10\sin(0.2t + 2\pi - 2), -10\cos(0.2t + 2\pi - 2), 0.2t - 2]^T$. The initial position and velocity are $\eta(0) = [-15, -15, 0]^T$, $\upsilon(0) = [0, 0, 0]^T$, respectively.

Table 1
Model parameters.

Items	Value	Items	Value
m	23.8000 kg	Y_v	−0.8897 kg/s
I_z	1.7600 kg m^2	$Y_{\|v\|v}$	−36.4729 kg/m
x_g	0.0460 m	$Y_{\|r\|v}$	−0.8050 kg/m
X_u	−0.7225 kg/s	Y_r	−7.2500 kg m/s
$X_{\|u\|u}$	−1.3274 kg/m	$Y_{\|v\|r}$	−0.8450 kg/m
$X_{\dot{u}}$	−2.0000 kg	$Y_{\|r\|r}$	−3.4500 kg/m
$Y_{\dot{v}}$	−10.0000 kg	$Y_{\dot{r}}$	0
N_v	0.0313 kg m^2/s	$N_{\|v\|v}$	3.9565 kg/m
$N_{\|r\|v}$	0.1300 kg/m	N_r	−1.9000 kg m^2/s
$N_{\|v\|r}$	0.0800 kg/m	$N_{\|r\|r}$	−0.7500 kg/m
$N_{\dot{r}}$	−1.0000 kg m^2		

The model uncertainties are selected as $M_\Delta = 0.2M_0$, $C_\Delta = 0.2C_0$ and $D_\Delta = 0.2D_0$. The environmental disturbance vector in this paper is divided into the following two cases:

• *Continuous type disturbance*. The disturbance vector is given by

$$\tau_d = \begin{bmatrix} 2\sin(0.08\pi t - \pi/6) + 0.5\cos(0.05\pi t + \pi/2) \\ 2\sin(0.08\pi t - \pi/3) + 0.5\cos(0.05\pi t + \pi/4) \\ 2\sin(0.08\pi t + \pi/2) + 0.5\cos(0.05\pi t + \pi/9) \end{bmatrix}$$

• *Step type disturbance*. The disturbance is represented by $d = J^T\zeta$ in the Earth-fixed frame. A frequently used bias model for marine control application is the 1st-order Markov process: (Fossen, 2011)

$$\dot{\zeta} = -A_\zeta^{-1}\zeta + B_\zeta\omega_\zeta$$

where $\omega_\zeta \in \mathbb{R}^3$ is the vector of the Gaussian white noise with zero mean value, A_ζ is the diagonal matrix of positive bias time constants, and B_ζ is a diagonal matrix scaling the amplitude of noise. The Band-Limited White Noise block with sample time 0.1 [s] and noise power $[10, 10, 100]$ generates the white noise in simulation. The initial value for bias is selected as $\zeta(0) = [-0.2, -0.5, 1]^T$. $A_\zeta = diag([100, 100, 100]^T)$, $B_\zeta = diag([0.04, 0.02, 0.03]^T)$.

The dynamic safety constraints in the position and velocity are designed as follows:

$$a_l = \begin{bmatrix} x_d - (2.5 + 5\exp(-0.2t))\,(1 - 0.2\cos(0.2t)) \\ y_d - (2.5 + 5\exp(-0.2t))\,(1 + 0.2\sin(0.2t)) \\ \psi_d - (0.5 - 0.2\exp(0.1t)) \end{bmatrix}$$

$$a_h = \begin{bmatrix} x_d - 2.5\,(1 - 0.2\sin(0.3t + 2)) \\ y_d - 2.5\,(1 + 0.2\cos(0.3t)) \\ \psi_d + (1 + 0.3\exp(-0.1t)) \end{bmatrix}$$

$$b_l = \begin{bmatrix} -0.1 - 0.5\exp(-0.2t) - 0.2\cos(0.1t) \\ -0.2\cos(0.09t + 2) - 3 \\ -0.35 - 0.75\exp(-0.5t) - 0.05\cos(0.1t) \end{bmatrix},$$

$$b_h = \begin{bmatrix} 3.5 + 0.5\exp(-0.4t) + 0.2\sin(0.1t) \\ 0.3 - 0.1\sin(0.09t + 2) \\ 0.35 + 0.25\exp(-0.1t) + 0.1\sin(0.1t) \end{bmatrix}.$$

The controller parameters are selected as $K_1 = \text{diag}([1, 1, 1]^T)$, $K_2 = \text{diag}([1, 1, 10]^T)$, $A_1 = 5$, $B_1 = 8$, $C_1 = 5$, $A_2 = 2$, $B_2 = 3$, $C_2 = 2$, $A_3 = 5$, $B_3 = 5.5$, $C_3 = 5$. The SMDO parameters are selected as $\rho_1 = \text{diag}([0.02, 0.02, 0.02]^T)$, $\rho_2 = \text{diag}([0.1, 0.2, 0.1]^T)$, $\rho_3 = \text{diag}([0.02, 0.02, 0.02]^T)$, $\rho_4 = \text{diag}([20, 30, 12]^T)$, $\rho_5 = \text{diag}([1, 2, 1]^T)$, $k_o = \text{diag}([0.9, 0.6, 0.6]^T)$. The initial values of the SMDO are $\hat{v} = [0, 0, 0]^T$ and $\beta = [-0.01, -0.01, -0.01]^T$.

The estimation results of two different types of lumped disturbances are shown in Figs. 1–2, respectively. As shown in Figs. 1–2, the SMDO can effectively estimate two different types of lumped disturbances. The motion of the DP ship in the horizontal plane is shown in Fig. 3. In Fig. 3, we can see that the trajectory tracking performance of the proposed is better than the method in Li et al. (2022a). The comparative trajectory tracking performances are shown in Figs. 4–5. In Fig. 4, the tracking performance of the proposed controller and the controller in Li et al. (2022a) keeps within the dynamic safety constraints. The position of the DP ship based backstepping method without UBF in three directions transcends the dynamic safety constraints at 1.8s. The

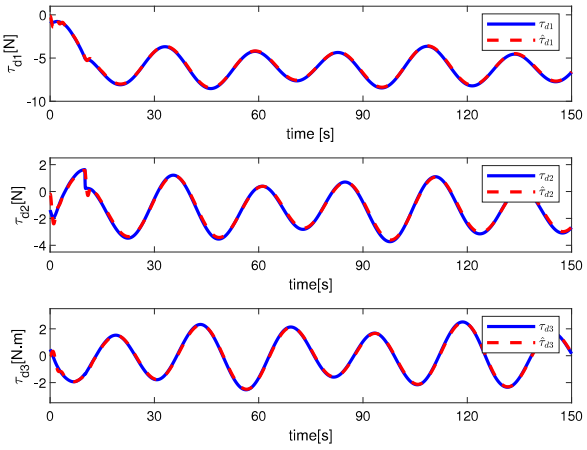

Fig. 1. The estimation of the lumped disturbances (Continuous type).

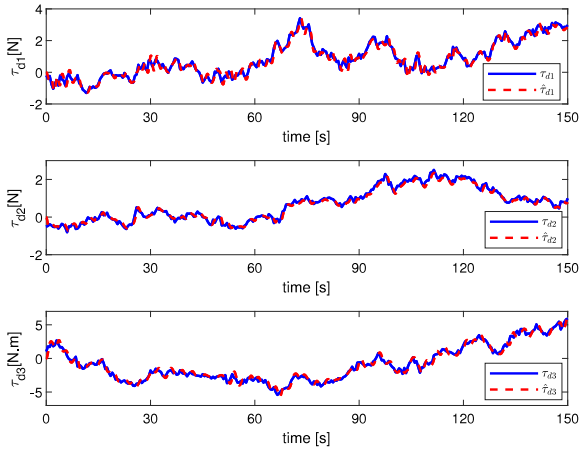

Fig. 2. The estimation of the lumped disturbances (Step type).

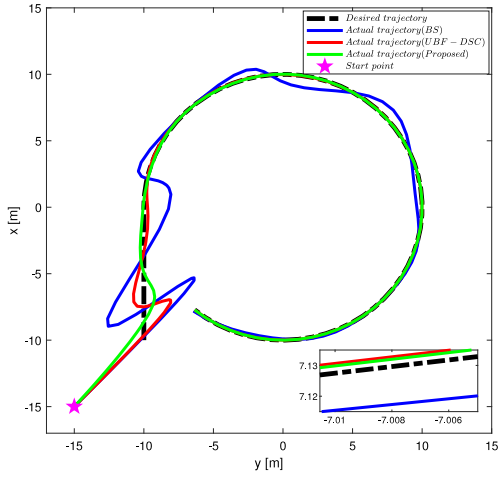

Fig. 3. The desired trajectory and actual trajectory of the DP ship with three differential control approaches.

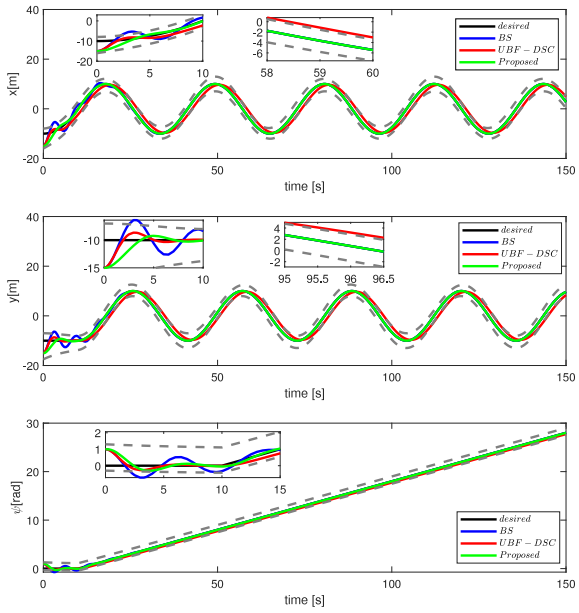

Fig. 4. The position of the DP ship under three differential control approaches.

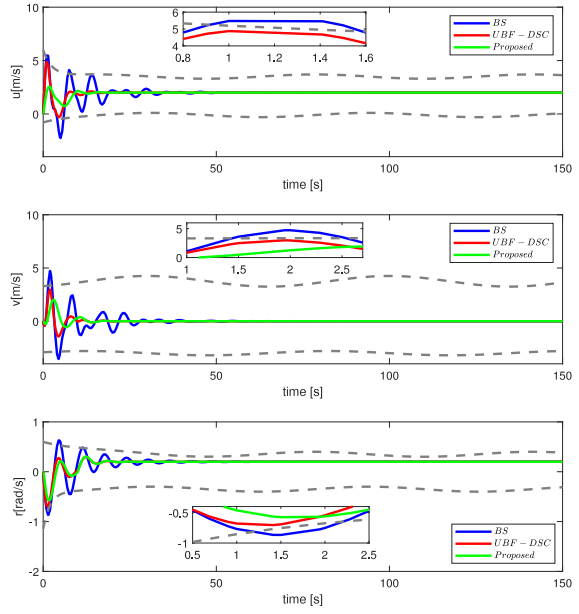

Fig. 5. The velocity of the DP ship under three differential control approaches.

velocities of the DP ship under three different control approaches are shown in Fig. 5. Due to the effect of the UBF, the velocities based on the proposed method and the method in Li et al. (2022a) keep within the dynamic safety constraints. The velocity based on the backstepping method without UBF in three directions transcends the dynamic safety constraints. The control input of the DP ship based on the proposed method is shown in Fig. 6. It is worth noting that, in comparison with Li et al. (2022a), the proposed method in this paper use the BNDM to smooth the virtual control force and limit the virtual control in a certain range, and solve velocity-jump issue, which can be verified by Figs. 3–6.

5. Conclusions

In this paper, a robust tracking control for dynamic positioning ships subject to dynamic safety constraints has been studied. The proposed

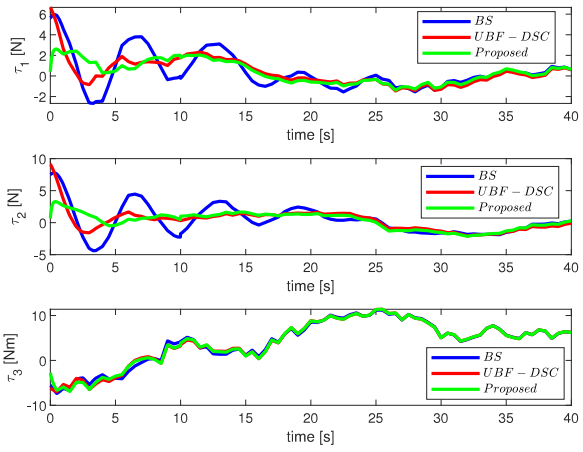

Fig. 6. The control input of the DP ship with three differential control approaches.

controller in conjunction with SMDO, UBF and BNDM can force the DP ship to achieve high-precision tracking performance. With UBF, the position and velocity of the DP ship can be rigorously kept within the dynamic safety constraints. In future work, the input saturation and control allocation of the DP ship will be considered.

CRediT authorship contribution statement

Yeye Liu: Writing – original draft, Conception and design of study, Writing – review & editing. **Xiaogong Lin:** Formal analysis, Analysis of data. **Kun Liang:** Funding acquisition, Acquisition of data.

Declaration of competing interest

The authors declare that they have no known competing financial interests or personal relationships that could have appeared to influence the work reported in this paper.

Data availability

No data was used for the research described in the article.

References

Chen, M., Chen, S., Wu, Q., 2017. Sliding mode disturbance observer-based adaptive control for uncertain MIMO nonlinear systems with dead-zone. Internat. J. Adapt. Control Signal Process. 31 (7), 1003–1018.

Dang, X., Truong, H., Do, V., 2022. A path planning control for a vessel dynamic positioning system based on robust adaptive fuzzy strategy. Automatika 63 (3), 580–592.

Du, J., Hu, X., Liu, H., Chen, C.P., 2015. Adaptive robust output feedback control for a marine dynamic positioning system based on a high-gain observer. IEEE Trans. Neural Netw. Learn. Syst. 26 (11), 2775–2786.

Fossen, T.I., 2011. Handbook of Marine Craft Hydrodynamics and Motion Control. John Wiley & Sons.

Ghommam, J., Saad, M., Mnif, F., 2022. Prescribed performances based fuzzy-adaptive output feedback containment control for multiple underactuated surface vessels. Ocean Eng. 249, 110898.

He, W., Yin, Z., Sun, C., 2016. Adaptive neural network control of a marine vessel with constraints using the asymmetric barrier Lyapunov function. IEEE Trans. Cybern. 47 (7), 1641–1651.

Kong, L., He, W., Yang, C., Li, G., Zhang, Z., 2018. Adaptive fuzzy control for a marine vessel with time-varying constraints. IET Control Theory Appl. 12 (10), 1448–1455.

Kulczycki, P., Korbicz, J., Kacprzyk, J., 2021. Automatic Control, Robotics, and Information Processing. Springer.

Li, H., Lin, X., 2022. Robust finite-time fault-tolerant control for dynamic positioning of ships via nonsingular fast integral terminal sliding mode control. Appl. Ocean Res. 122, 103126.

Li, H., Lin, X., Jiang, A., Lai, C., 2022a. Control allocation-based robust tracking control for overactuated surface vessels subject to time-varying full-state constraints. Electronics 11 (5), 794.

Li, J., Xiang, X., Yang, S., 2022b. Robust adaptive neural network control for dynamic positioning of marine vessels with prescribed performance under model uncertainties and input saturation. Neurocomputing 484, 1–12.

Lu, J., Yu, S., Zhu, G., Zhang, Q., Chen, C., Zhang, J., 2021. Robust adaptive tracking control of UMSVs under input saturation: A single-parameter learning approach. Ocean Eng. 234, 108791.

Mu, D.D., Wang, G.F., Fan, Y.S., 2018. Tracking control of podded propulsion unmanned surface vehicle with unknown dynamics and disturbance under input saturation. Int. J. Control Autom. Syst. 16 (4), 1905–1915.

Pan, C.Z., Lai, X.Z., Yang, S.X., Wu, M., 2015. A biologically inspired approach to tracking control of underactuated surface vessels subject to unknown dynamics. Expert Syst. Appl. 42 (4), 2153–2161.

Qiao, L., Zhang, W., 2017. Adaptive non-singular integral terminal sliding mode tracking control for autonomous underwater vehicles. IET Control Theory Appl. 11 (8), 1293–1306.

Qiao, L., Zhang, W., 2018. Double-loop integral terminal sliding mode tracking control for UUVs with adaptive dynamic compensation of uncertainties and disturbances. IEEE J. Ocean. Eng. 44 (1), 29–53.

Qiao, L., Zhang, W., 2019. Trajectory tracking control of AUVs via adaptive fast nonsingular integral terminal sliding mode control. IEEE Trans. Ind. Inf. 16 (2), 1248–1258.

Qin, H., Li, C., Sun, Y., Li, X., Du, Y., Deng, Z., 2020. Finite-time trajectory tracking control of unmanned surface vessel with error constraints and input saturations. J. Franklin Inst. B 357 (16), 11472–11495.

Riani, A., Madani, T., Benallegue, A., Djouani, K., 2018. Adaptive integral terminal sliding mode control for upper-limb rehabilitation exoskeleton. Control Eng. Pract. 75, 108–117.

Sariyildiz, E., Oboe, R., Ohnishi, K., 2019. Disturbance observer-based robust control and its applications: 35th anniversary overview. IEEE Trans. Ind. Electron. 67 (3), 2042–2053.

Skjetne, R., Fossen, T.I., Kokotović, P.V., 2005. Adaptive maneuvering, with experiments, for a model ship in a marine control laboratory. Automatica 41 (2), 289–298.

Sun, T., Cheng, L., Wang, W., Pan, Y., 2020. Semiglobal exponential control of Euler–Lagrange systems using a sliding-mode disturbance observer. Automatica 112, 108677.

Sun, Z., Zhang, G., Yang, J., Zhang, W., 2018. Research on the sliding mode control for underactuated surface vessels via parameter estimation. Nonlinear Dynam. 91 (2), 1163–1175.

Tee, K.P., Ge, S.S., 2011. Control of nonlinear systems with partial state constraints using a barrier Lyapunov function. Internat. J. Control 84 (12), 2008–2023.

Van, M., 2019. An enhanced tracking control of marine surface vessels based on adaptive integral sliding mode control and disturbance observer. ISA Trans. 90, 30–40.

Wang, D., Ge, S.S., Fu, M., Li, D., 2021. Bioinspired neurodynamics based formation control for unmanned surface vehicles with line-of-sight range and angle constraints. Neurocomputing 425, 127–134.

Wei, X., You, L., Zhang, H., Hu, X., Han, J., 2022. Disturbance observer based control for dynamically positioned ships with ocean environmental disturbances and actuator saturation. Internat. J. Robust Nonlinear Control 32 (7), 4113–4128.

Yang, S.X., Zhu, A., Yuan, G., Meng, M.Q.-H., 2011. A bioinspired neurodynamics-based approach to tracking control of mobile robots. IEEE Trans. Ind. Electron. 59 (8), 3211–3220.

Zhang, H., Zhang, X., Bu, R., 2022. Sliding mode adaptive control for ship path following with sideslip angle observer. Ocean Eng. 251, 111106.

Zhao, K., Song, Y., Chen, C.P., Chen, L., 2020. Control of nonlinear systems under dynamic constraints: A unified barrier function-based approach. Automatica 119, 109102.

Zheng, Z., Su, X., Jiang, T., Huang, J.-S., 2022b. Robust dynamic geofencing attitude control for quadrotor systems. IEEE Trans. Ind. Electron..

Zheng, Y., Tao, J., Sun, Q., Sun, H., Chen, Z., Sun, M., Xie, G., 2022a. Soft actor–critic based active disturbance rejection path following control for unmanned surface vessel under wind and wave disturbances. Ocean Eng. 247, 110631.